Biogeophysical feedback of phytoplankton on Arctic climate. Part II: Arctic warming amplified by interactive chlorophyll under greenhouse warming

Hyung-Gyu Lim, Jong-Seong Kug & Jong-Yeon Park

Climate Dynamics
Observational, Theoretical and Computational Research on the Climate System

ISSN 0930-7575
Volume 53
Combined 5-6

Clim Dyn (2019) 53:3167-3180
DOI 10.1007/s00382-019-04693-5

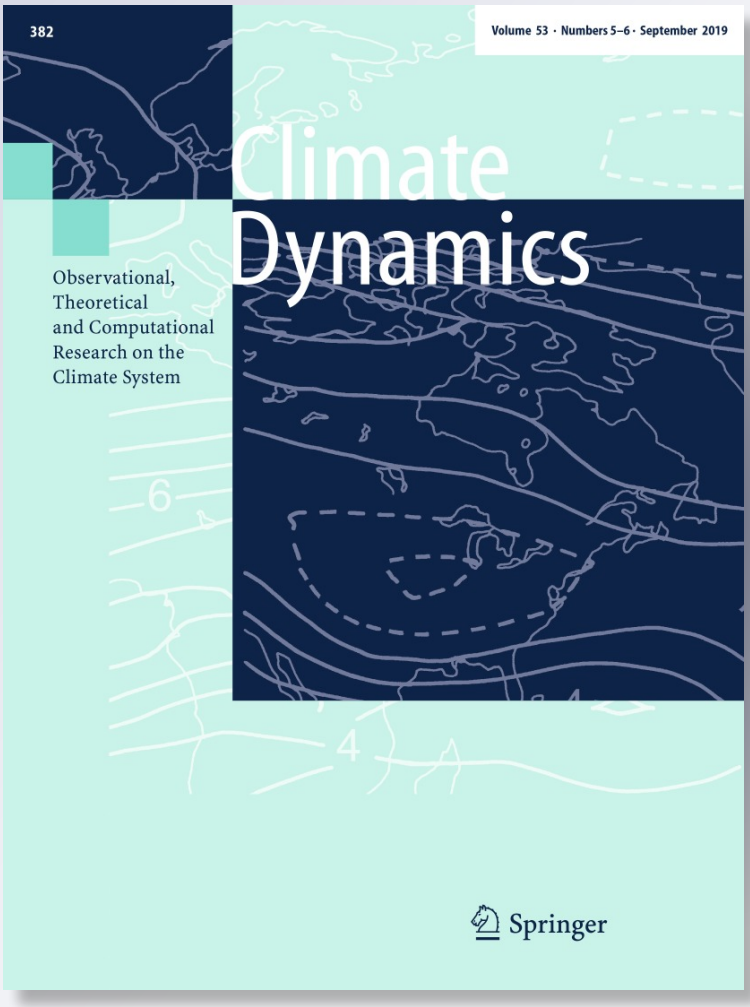

Springer

Climate Dynamics (2019) 53:3167–3180
https://doi.org/10.1007/s00382-019-04693-5

Biogeophysical feedback of phytoplankton on Arctic climate. Part II: Arctic warming amplified by interactive chlorophyll under greenhouse warming

Hyung-Gyu Lim[1] · Jong-Seong Kug[1] · Jong-Yeon Park[2]

Received: 8 August 2018 / Accepted: 18 February 2019 / Published online: 1 March 2019

Abstract
It has been shown that the interaction between marine phytoplankton and climate systems may intensify Arctic warming in the future via shortwave heating associated with increased spring chlorophyll bloom. However, the changes of chlorophyll variability and its impact on the Arctic future climate are uncomprehended. Lim et al. (Clim Dyn. https://doi.org/10.1007/s00382-018-4450-6, 2018a) (Part I) suggested that two nonlinear rectifications of chlorophyll variability play cooling role in present-day climate. In this study, we suggest that the decreased interannual chlorophyll variability may amplify Arctic surface warming (+ 10% in both regions) and sea ice melting (− 13% and − 10%) in Kara-Barents Seas and East Siberian-Chukchi Seas in boreal winter, respectively. Projections of earth system models show a future decrease in chlorophyll both mean concentration and interannual variability via sea ice melting and intensified surface-water stratification in summer. We found that suggested two nonlinear processes in Part I will be reduced by about 31% and 20% in the future, respectively, because the sea ice and chlorophyll variabilities, which control the amplitudes of nonlinear rectifications, are projected to decrease in the future climate. The Arctic warming is consequently enhanced by the weakening of the cooling effects of the nonlinear rectifications. Thus, this additional biological warming will contribute to future Arctic warming. This study suggests that effects of the mean chlorophyll and its variability should be considered to the sensitivity of Arctic warming via biogeophysical feedback processes in future projections using earth system models.

Keywords Chlorophyll variability · Arctic amplification · Bio-optical effect · Biogeochemical model · Biogeophysical feedback · Ice–phytoplankton coupling

1 Introduction

The body of existing research has clearly shown that global warming reduces the extent and thickness of sea ice based on satellite observations in the Arctic (Comiso 2003; Maslanik et al. 2007; Serreze et al. 2007; Min et al. 2015) and future projections by climate models (Boé et al. 2009; Stroeve et al. 2012; Liu et al. 2013; Overland and Wang 2013). Under current conditions, Arctic warming is amplified by positive ice–albedo feedback (Perovich et al. 2007; Holland et al. 2010; Kashiwase et al. 2017), where transmission of surface shortwave flux on the Arctic Ocean surface is increased with shrinking sea ice, which contributes to the warming of the Arctic ocean (Perovich et al. 2011; Nicolaus et al. 2012; Arrigo et al. 2014).

The increased penetration of shortwave flux through the shrinking sea ice induces changes in the Arctic ecosystem (Wassmann and Reigstad 2011; Doney et al. 2012; Winder and Sommer 2012). The timing of phytoplankton spring bloom in a future climate becomes earlier due to earlier melting of sea ice than that in the present climate (Wassmann and Reigstad 2011; Arrigo et al. 2012; Ardyna et al. 2014; Frey et al. 2015). In the long term, the stratification of surface ocean water is intensified globally by greenhouse warming (Sarmiento et al. 2004; Behrenfeld et al. 2006; Bopp et al. 2013), but particularly in the Arctic Ocean (Vancoppenolle et al. 2013; Lawrence et al. 2015; Peralta-Ferriz

✉ Jong-Seong Kug
jskug1@gmail.com

[1] Division of Environmental Science and Engineering, Pohang University of Science and Technology (POSTECH), 77 cheongam-Ro Nam-Gu, Pohang 790-784, South Korea

[2] Department of Earth and Environmental Sciences, Chonbuk National University, Jeonju, South Korea

and Woodgate 2015; Dunstan et al. 2018). The stratification by greenhouse warming contributes to the decreasing trend in the nutrient inventory and phytoplankton biomass in the Arctic Ocean (Boyce et al. 2010; Cabré et al. 2015).

It has been suggested that Arctic phytoplankton may play a role in controlling Arctic climate sensitivity to anthropogenic greenhouse warming (Park et al. 2015). The chlorophyll, which is indicative of phytoplankton biomass, absorbs shortwave radiation on the ocean surface and modulates the oceanic vertical thermal structure. This process allows for the two-way interaction between physics and biogeochemistry, or so-called biogeophysical feedback (Morel 1988; Morel and Antoine 1994; Manizza et al. 2005; Lengaigne et al. 2007). Earth system model (ESM) experiments simulating these biogeophysical feedbacks have suggested that biogeophysical feedback has a warming effect in terms of the mean chlorophyll concentration (Lengaigne et al. 2009; Park et al. 2015). Using a IPSL-CM4 model, Lengaigne et al. (2009) demonstrated that greater mean chlorophyll concentration leads to warmer sea surface temperature and reduction of ice concentration in the present climate because of more shortwave flux absorption in the surface layer. Under greenhouse warming conditions, Park et al. (2015), using GFDL-CM2.1 and MPI-ESM models, demonstrated that increased mean chlorophyll concentrations in spring associated with early sea ice melting absorbs more shortwave flux and amplifies Arctic warming.

While Lengaigne et al. (2009) and Park et al. (2015) highlighted the impact of mean chlorophyll concentration on Arctic present and future climate, Lim et al. (2018a) (hereinafter Part I) pointed out that the presence of interannual interactive chlorophyll variability also has a distinctive impact on the Arctic climate, where interactive chlorophyll means that chlorophyll is computed in a biogeochemical model coupled with physical variables, and it gives a feedback to physical variables by altering shortwave absorption.

The first of these mechanisms is the cooling effect associated with nonlinear term of shortwave heating (NT_{sw}). In boreal summer, higher sea ice concentration, reflecting the shortwave radiation and increasing the salinity via brine rejection, enhances the ocean mixing. Subsequently, surface nitrate is enriched via enhanced ocean mixing. Therefore, the increased nitrate grows well the chlorophyll on the ocean surface in a condition of the higher sea ice concentration compared to the lower sea ice concentration in summer. As the higher sea ice concentration reflects more shortwave radiation, relationship between shortwave flux and chlorophyll variabilities is negative in summer, introduced as ice–phytoplankton coupling in Part I. Meanwhile, the shortwave absorption rate (α_{sw}) is positively proportional to chlorophyll concentration (Manizza et al. 2005). Consequently, positive ice–phytoplankton coupling is associated with the negative covariability between shortwave flux and α_{sw} variabilities, which leads to nonlinear cooling represented by the term NT_{sw} ($\overline{\alpha'_{sw} \times swflx'}$).

The second mechanism is the cooling effect due to the nonlinear function of the shortwave absorption rate (NF_{α}). The chlorophyll variability itself reduces time mean of the shortwave absorption rate ($\overline{\alpha_{sw}}$). Because, increasing amount of $\alpha_{sw,}$ increased by chlorophyll, is followed by the e-folding depth of shortwave attenuation ($1 - \exp^{-[chl]}$). In other words, the change in decaying slope of α_{sw} is nonlinear against increasing chlorophyll. Thus, given that the chlorophyll concentration is fixed, the $\overline{\alpha_{sw}}$ in the case of existing chlorophyll variability is always smaller than $\overline{\alpha_{sw}}$ in the case of fixed chlorophyll concentration. It always generates negative $\mathbf{\Delta}\overline{\alpha_{sw}}$ in the presence of interannual chlorophyll variability. This implies that the cooling effect of the rectification by NF_{α} is due to temporal variation in chlorophyll. These two nonlinear rectification effects of NT_{sw} and NF_{α} play important roles in the modulation of the Arctic climate mean state.

The suggested nonlinear rectification effects of interactive chlorophyll variability in the present-day climate may change in the future. For instance, the loss of summer sea ice in the future may reduce oceanic mixing due to the thermodynamic effect and freshwater flux related to sea ice melting (Cabré et al. 2015). These changes can affect the ice–phytoplankton coupling and in turn chlorophyll variability itself, which eventually may modulate Arctic climate sensitivity according to effects of NT_{sw} and NF_{α}. In this study, we highlight the seasonal dependency of mean chlorophyll changes, ice–phytoplankton coupling changes, and their climate effects in the future. The purpose of this work (Part II) is to revisit the previous work (i.e., Park et al. 2015, hereinafter, P15), and further investigate the detailed mechanism of Arctic warming amplified by the interactive chlorophyll in a future climate, while Part I focused on understanding the feedback in the present-day climate.

2 Model experiments

This study used a fully coupled model (version CM2.1) with an oceanic biogeochemical (BGC) model (Tracers of Phytoplankton with Allometric Zooplankton version 2, TOPAZv2) developed by the Geophysical Fluid Dynamics Laboratory (GFDL) (Griffies 2012; Dunne et al. 2013). This model was based on the open source code provided by the National Oceanic and Atmospheric Administration (NOAA, https://www.gfdl.noaa.gov/), which is a similar model configuration reported in Lim et al. (Lim et al. 2018a, b).

Four different experiments were conducted using this model. Under present-day climate conditions (i.e., fixed CO_2 concentrations at 1990 levels of 353 ppm), the CM2.1 was integrated by running the BGC model for 450 years after a 550-year spin-up (BGC.on.1×CO_2). This bio-climate

fully-coupled experiment simulates interactive chlorophyll variability via interaction between biogeochemical and climate model. In addition, the model was modified by turning off the BGC model for 250 years, and instead, three dimensions (longitude, latitude, and depth) for chlorophyll monthly climatology obtained from BGC.on were used for the model (BGC.off.1×CO_2). Therefore, in this experiment (BGC.off.1×CO_2), chlorophyll does not have interannual variability. These two experiments were also used in investigating the impact of interactive chlorophyll variability in Part I.

Under greenhouse warming conditions (i.e., CO_2 concentration increased by 1% per year to double from 353 ppm), the CM2.1 coupled with the BGC model is integrated for 200 years (BGC.on.2×CO_2). To obtain robust results, three ensemble members were integrated from three initial conditions after 550-, 800-, and 1000-year spin-ups of BGC.on.1×CO_2. Also, the model was integrated by turning off the BGC model for 200 years from the same three initial conditions of BGC.on.2×CO_2 (BGC.off.2×CO_2). The three-dimensional chlorophyll concentration was prescribed from monthly climatology of BGC.on.1×CO_2.

This study (i.e., Part II) re-examines the Arctic warming amplified by interactive chlorophyll. These four experimental designs were similar to the model configuration used in P15, but the updated version of the model (from MOM4 to MOM5) and oceanic BGC model (from TOPAZv1 to TOPAZv2) were used, and it has been further adjusted by about 100 years more integrations for the future climate than P15. All results were evaluated during the last 100 years to investigate Arctic climate sensitivity at an equilibrium state for CO_2. A summary of the four experiments is presented in Table 1. The changes of chlorophyll and shortwave heating terms are calculated in 30-m depth like as P15 to represent changes of upper ocean layer.

To investigate biogeophysical feedback, all experiments used the same shortwave heating scheme (Manizza et al. 2005). This scheme considers the attenuation coefficients modulated by the chlorophyll concentration in horizontal and vertical grids. The visible bands of the shortwave flux, partitioned between red and blue/green bands, were assumed to penetrate ocean waters down to the cutoff depth (200-m) to cover euphotic zone. In this case, the attenuation coefficients of the visible bands can be determined by the vertical profile of a simulated or prescribed chlorophyll concentration. This scheme allows for the computation of the biogeophysical feedback in every integration time and at a global scale in CM2.1.

3 Results

3.1 Seasonal variation of chlorophyll response in the future climate

Prior to examining the impact of interactive chlorophyll, we first checked the seasonal chlorophyll response under greenhouse warming conditions compared to present-day climate. Figure 1 shows the difference between seasonal mean chlorophyll concentrations in BGC.on.2×CO_2 and BGC.on.1×CO_2. In the Arctic Ocean, the change in chlorophyll concentrations under greenhouse warming is greater during boreal spring [March–May (MAM)] and summer [June–August (JJA)], while chlorophyll response is relatively weaker in boreal autumn [September–November (SON)] and winter [December–February (DJF)]. Interestingly, strong seasonal dependency in chlorophyll response was observed, increasing in MAM and decreasing in JJA. The magnitude of chlorophyll response in JJA (− 0.16 mg/m^3) was larger than in MAM (+0.07 mg/m^3) in the Arctic Ocean (65°–90°N, all longitudes). Since the summer response was greater than the spring response, the annual mean Arctic chlorophyll was reduced by about 0.03 mg/m^3 in the future Arctic climate compared to the present-day. Annual mean chlorophyll decrease was also simulated in the mean of multi-model ensemble of ESM simulations from the recent Coupled Model Intercomparison Project (CMIP5) in future projections (Cabré et al. 2015).

In P15, it was argued that spring chlorophyll will increase due to sea ice reduction, which will enhance the availability of light. In Part I, this relationship was demonstrated by the negative correlation coefficient between sea ice and

Table 1 Summary of experiments used in this study

Exp.	Model	Chlorophyll concentration	Simulated period
BGC.on.1×CO_2	CM2.1 + TOPAZ2	Simulated	450 years after 550 year spin-up
BGC.on.2×CO_2	”	”	200 years × 3 after 550, 800, 1000 year spin-up of BGC.on.1×CO_2
BGC.off.1×CO_2	CM2.1	Global monthly climatology of BGC.on.1×CO_2	250 years after 550 year spin-up
BGC.off.2×CO_2	”	”	200 years × 3 after 551, 800, 1000 year spin-up of BGC.on.1×CO_2

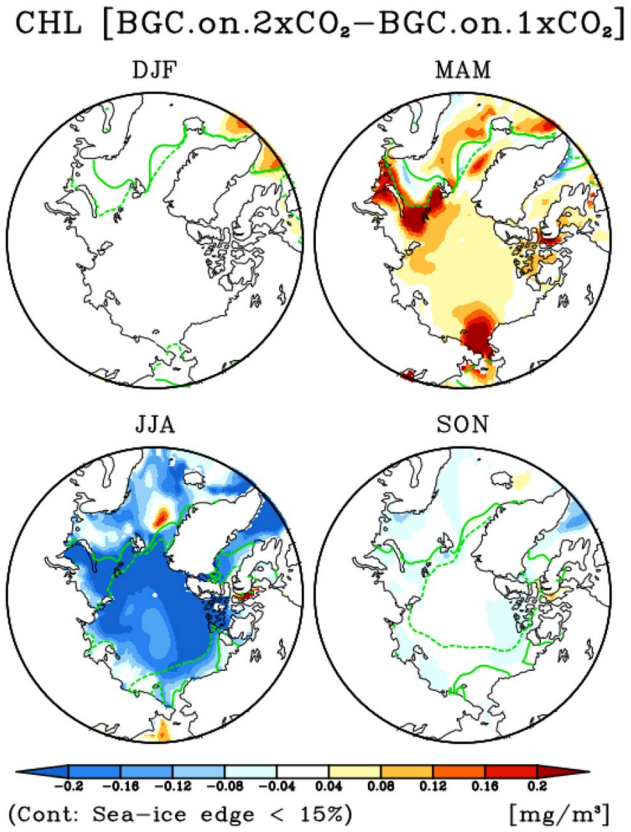

Fig. 1 Mean seasonal differences in the simulated chlorophyll concentration between the present-day (BGC.on.1×CO_2) and future climate (BGC.on.2×CO_2) averaged up to 30-m depth of the ocean. Contour lines denote the sea ice edge (defined as the location where sea ice fraction reaches 15%). Solid and dashed lines correspond to the present-day and future climates, respectively. *MAM* March–May, *JJA* June–August, *SON* September–November, *DJF* December–February

chlorophyll concentration anomalies in spring. Thus, sea ice melting under greenhouse warming conditions induces an increase in chlorophyll in spring. In these experiments, the sea ice edge (< 15% of sea ice concentration) is shrunk 14% from the present-day climate (16.9 Million km^2; straight green line in Fig. 1) to the future climate (14.5 Million km^2; dashed green line in Fig. 1) in MAM. Under these conditions, spring chlorophyll levels, which are primarily controlled by shortwave flux, can be increased (Arrigo et al. 2008; Wassmann and Reigstad 2011; Popova et al. 2012). This increasing chlorophyll response is stronger in the East Siberian-Chukchi Seas (160°E–160°W, 65°–80°N) and Barents-Kara Seas (30°–70°E, 70°–80°N), which matches well with the increased chlorophyll pattern in P15.

In contrast to the spring case, the summer chlorophyll decreases under greenhouse warming conditions, which is also consistent with P15. This decreasing chlorophyll is also related to sea ice reduction. This relationship was demonstrated in Part I by the strong positive correlation coefficient between sea ice and chlorophyll concentration anomalies in summer. Because sea ice reflects shortwave radiation and in turn reduces the shortwave heating on the ocean surface, the presence of sea ice reduces the stratification of surface ocean water. Under greenhouse warming conditions, the surface of the Arctic Ocean will be stratified by melting sea ice, which will enhance nutrient depletion, leading to a decrease in chlorophyll levels. In the present experiments, the sea ice edge was shrunk 45% from present-day climate (8.19 Million km^2) to the future climate (4.52 Million km^2) in JJA. In this condition, summer chlorophyll will decrease because it is primarily controlled by nitrate concentrations (Tremblay and Gagnon 2009; Vancoppenolle et al. 2013).

To further investigate the chlorophyll response mechanism in future projections, the vertical structures of density, temperature, salinity, nitrate, and chlorophyll in Arctic Ocean are shown in Fig. 2. In present-day climate, the climatologies of pycnocline, thermocline, and halocline closely affect nutrient entrainment from the subsurface to the surface (contours in Fig. 2a–c). Since the seasonal cycle of sea ice is at a minimum in summer, the low density and warm conditions of the surface ocean water are at their highest in summer due to the relatively larger input of fresh water and shortwave radiation. The surface salinity was also at its lowest in summer due to the largest fresh water flux associated with the thawing season. These seasonal cycles in summer induce the steepest stratification in summer, which prevents vertical mixing in the upper ocean layer. The nutrient entrainment from the sufficient nutrient inventory in the subsurface to the surface ocean decreases in summer. Thus, the nutricline (contour in Fig. 2d) will generally follow the deepening of the pycnocline, thermocline, and halocline. The depth of the subsurface chlorophyll maximum in spring moves to the deeper ocean in summer following the deepening of the nutricline (contour in Fig. 2e).

Under greenhouse warming conditions, the oceanic stability is increased, which is maximized in May (shading in Fig. 2a). The reduction of sea ice concentrations allows more input of shortwave flux, which enhances the ocean surface warming and deepens thermocline depth (shading in Fig. 2b). Furthermore, the sea ice melting releases fresh water into the sea water, which reduces surface salinity and deepens halocline depth in the upper ocean (shading in Fig. 2c). These two physical processes, surface warming and freshening, reduce surface-water density and induce stronger oceanic stability, which inevitably leads to nutrient depletion (shading in Fig. 2d). In addition, the nutrient depletion is associated with biological process under greenhouse warming. The increased chlorophyll concentration in spring, which is maximized in May to a depth 30-m, will spend more nutrient inventory. The depth of the subsurface chlorophyll maximum is moved to deeper ocean due to reduced nitrate concentration of Arctic ocean surface in summer. Consequently, the summer chlorophyll up to 30-m depth

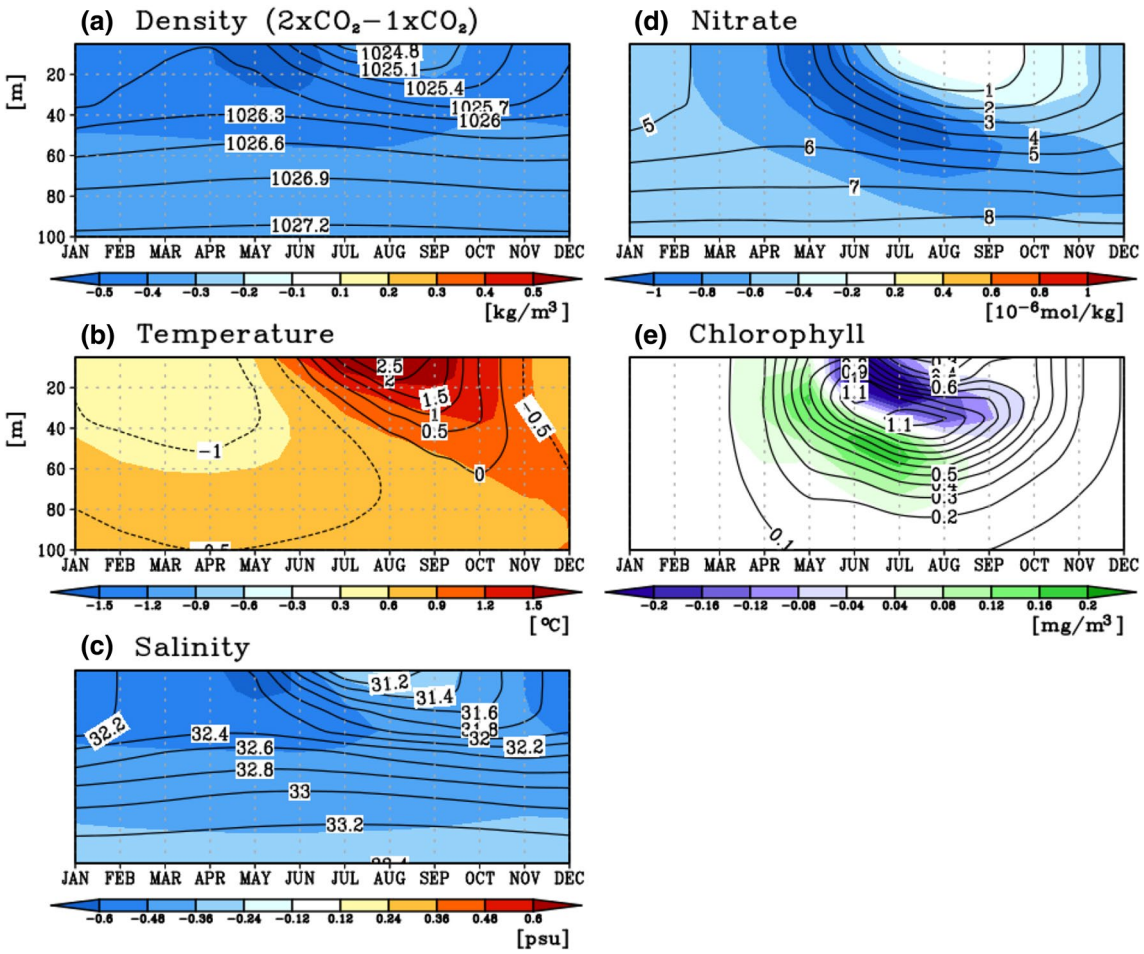

Fig. 2 Vertical structures of monthly climatologies of present-day (BGC.on.1×CO_2; contour) and differences between the present-day and future climates (BGC.on.2×CO_2 minus BGC.on.1×CO_2; shading) of the simulated **a** density, **b** temperature, **c** salinity, **d** nitrate, and **e** chlorophyll in the Arctic Ocean (> 65°N)

will be reduced by nutrient depletion at the surface under greenhouse warming conditions (shading in Fig. 2e). The chlorophyll response displays strong seasonal dependency, resulting in increased chlorophyll in MAM and decreased chlorophyll in JJA, due to light limiting conditions in MAM and nutrient-limiting conditions in JJA.

3.2 Impact of interactive chlorophyll on the Arctic warming

In general, the concentration of chlorophyll determines the shortwave attenuation coefficients with larger chlorophyll concentrations enhancing the shortwave absorption rate in the upper ocean. (Manizza et al. 2005). Thus, an increase in spring chlorophyll concentrations can absorb more shortwave radiation, while a decrease in summer chlorophyll concentrations would absorb less shortwave radiation. Given a decrease in annual mean chlorophyll, it is expected that the biogeophysical feedback will reduce absorption of shortwave flux, which attenuates Arctic amplification under greenhouse warming conditions.

Surprisingly, however, Arctic warming is amplified by interactive chlorophyll under greenhouse warming conditions. Figure 3a shows the biologically-induced responses of sea ice and surface temperature estimated by the difference between two sets of future (2×CO_2) and present-day (1×CO_2) climate runs [i.e., (BGC.on.2×CO_2 − BGC.off.2×CO_2) − (BGC.on.1×CO_2 − BGC.off.1×CO_2)]. The interactive chlorophyll and its biogeophysical feedback on the Arctic induce the additional warming of surface temperature (contour in Fig. 3a). These warming patterns of interactive chlorophyll runs (BGC.on.2×CO_2 − BGC.on.1×CO_2) were observed in all seasons compared to non-interactive chlorophyll runs (BGC.off.2×CO_2 – BGC.off.1×CO_2), while weak cooling was observed over Greenland and Fram Strait. The warming is strongest in the East Siberian-Chukchi Seas (160°E–160°W, 65°–80°N) at about 0.9 °C (+ 10%) and the Barents-Kara Seas (30°–70°E, 70°–80°N) at about 1.2 °C

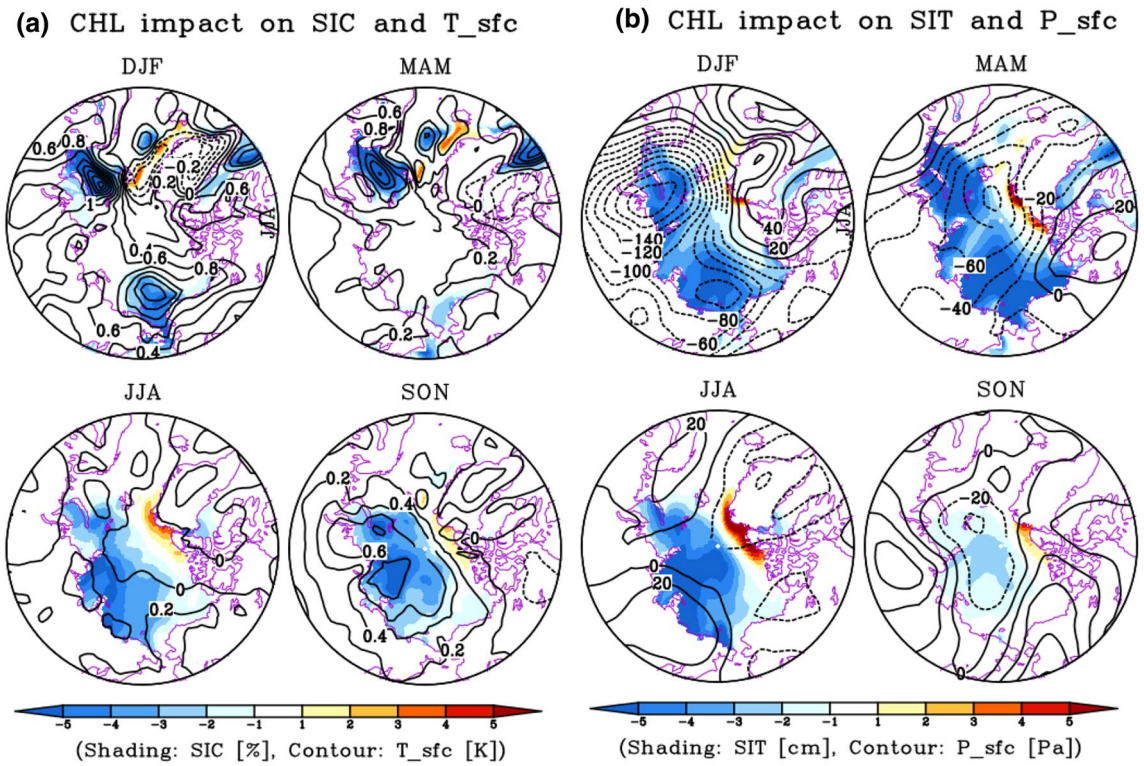

Fig. 3 The chlorophyll impact on seasonal **a** sea ice concentration (SIC; shading) and surface temperature (T_sfc; contour), **b** sea ice thickness (SIT; shading) and surface pressure (P_sfc; contour). *MAM* March–May, *JJA* June–August, *SON* September–November, *DJF* December–February. Chlorophyll impact is estimated by a set of future climate experiments [BGC.on.2×CO_2 minus BGC.off.2×CO_2] minus a set of present-day climate experiments [BGC.on.1×CO_2 minus BGC.off.1×CO_2]

(+ 13%) in DJF and the strongest in the Laptev-Kara Seas at about 0.6 °C (+ 13%) (50°–150°E, 70°–80°N) in SON.

In general, the biologically-induced Arctic sea ice concentration (shading in Fig. 3a) and thickness (shading in Fig. 3b) represent additional reductions in all seasons. While the sea ice thickness decreases in both the Eurasian and Amerasian Basins of the Arctic Ocean (30°–160°W, 65°–90°N) by about − 3.7 cm (− 15%) during months, the reductions of sea ice concentration show seasonal dependency along with marginal ice zone. The reduction in the sea ice concentration is the highest in the East Siberian-Chukchi Seas at about − 3.0% (− 10%) and Barents-Kara Seas at about − 4.7% (− 13%) in DJF; highest in the Laptev-Kara Seas at about − 3.7% (− 15%) in SON. The biologically-induced reductions of sea ice concentration and sea ice thickness enhance ice–albedo feedback (Perovich et al. 2007; Holland et al. 2010; Kashiwase et al. 2017), which amplifies the Arctic warming patterns.

In addition, the weak sea ice freezing patterns are observed near East Greenland in DJF and North Greenland in JJA. These freezing patterns are associated with the dipole pattern of surface pressure (contour in Fig. 3b). The sea ice melting in winter generates expansion of the open ocean, which warms the cold air in winter. The surface pressure is then gradually reduced in surface temperature warming regions, with the lowest observed in the East Siberian-Chukchi Seas and Barents-Kara Seas in DJF, while surface pressure is increased by about 35 Pa over West Greenland and the Canadian Arctic Archipelago (90°–30°E, 65°–80°N) in DJF (contour in Fig. 3b). This Arctic dipole pattern, a negative anomaly in the Barents-Kara Seas and a positive anomaly in the Arctic Archipelago, enhances the Transpolar Drift Stream (Wang et al. 2009). This can move the thinned sea ice, with an increased mobility and outflow via the Fram Strait (Haas et al. 2008; Kwok and Rothrock 2009; Wang et al. 2009), which may induce slight increases in the sea ice over East Greenland (Comiso et al. 2008; Deser and Haiyan 2013).

In boreal winter and spring, sea ice reductions are generally manifested in the Chukchi and Barents Seas where the spring mean chlorophyll concentration is increased. This sea ice melting should be associated with increased mean chlorophyll, which can absorb more shortwave radiation. In boreal summer and fall, sea ice reductions are also manifested in the Kara, Laptev and East Siberian Seas where the summer mean chlorophyll concentration is decreased. To understand how much interactive chlorophyll feedback enhances solar energy, the biologically-induced shortwave

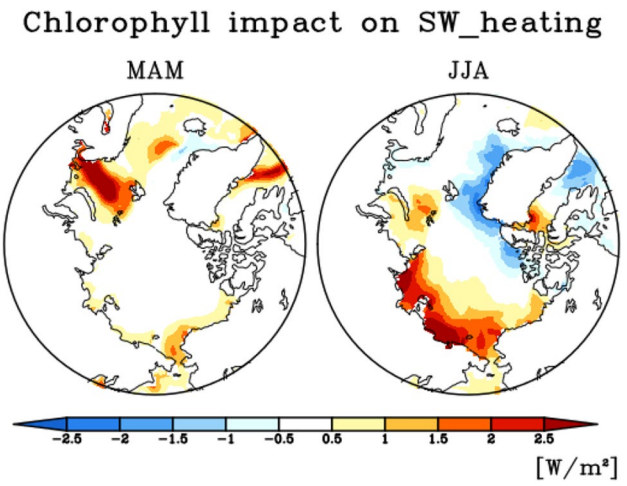

Fig. 4 The impact of interactive chlorophyll on shortwave heating from March to May (MAM; left) and from June to August (JJA; right) up to 30 m of the Arctic Ocean

heating is compared in the surface layer of the Arctic Ocean. As shown in Fig. 4, both spring and summer shortwave heating responses increase. In spring, the biologically-induced shortwave heating is strongest at about 2.4W/m^2 in the Barents Sea (30°–50°E, 70°–80°N) where the spring chlorophyll is significantly increased, while the autumn and winter shortwave heating responses are virtually zero (not shown). In summer, the biologically-induced shortwave heating is strongest at about 2.1 W/m^2 in the Laptev-East and Siberian-Chukchi Seas (70°E–160°W, 65°–75°N) where the summer chlorophyll is reduced, while shortwave cooling is observed along Greenland's coasts due to increases in sea ice concentration and thickness. The annual mean shortwave heating in the pan-Arctic Ocean is increased by about 0.2W/m^2 by biogeophysical feedback, which does not match well with decreased annual mean Arctic chlorophyll, as mentioned in Sect. 3.1. This mismatch between decreased mean chlorophyll and increased shortwave heating suggests that the existence of additional shortwave heating source of interactive chlorophyll, rather than associated mean chlorophyll change, amplifies the Arctic warming under greenhouse warming.

3.3 Suppression of nonlinear chlorophyll feedback in the future climate

In previous sections, we showed that the interactive chlorophyll has significant positive shortwave heating and in turn the warming effect on the future Arctic climate despite decreased mean chlorophyll concentration. In order to understand the warming effect physically, it should be addressed how the nonlinear chlorophyll feedback contributes to amplify the Arctic warming in a future climate.

To address this issue, we examine the partial shortwave heating terms as shown in Part I. The shortwave heating is controlled by the multiplication of α_{sw} and the input of shortwave flux (swflx) reaching on the ocean. The α_{sw} can be divided by the climatological monthly mean ($\overline{\alpha_{sw}}$) and the interannual monthly anomaly (α'_{sw}). The shortwave flux can also be divided by the climatological monthly mean ($\overline{swflx}$), and interannual monthly anomaly ($swflx'$). Thus, the difference in the time mean of shortwave heating as $\overline{\alpha_{sw} \times swflx}$ can be divided by mean and nonlinear parts of shortwave heating term as follows:

$$\overline{\alpha_{sw} \times swflx} = \overline{\overline{\alpha_{sw}} \times \overline{swflx}} + \overline{\alpha'_{sw} \times swflx'}$$

where, $\overline{\overline{\alpha_{sw}} \times \overline{swflx}}$ is the mean of mean shortwave heating (MMSH) and $\overline{\alpha'_{sw} \times swflx'}$ is the mean of the nonlinear shortwave heating (MNSH).

Part I suggested that MMSH and MNSH terms give significant cooling effects associated with two nonlinear rectifications of interactive chlorophyll variability in the present-day climate. One was NT_{sw}, estimated by MNSH term expressed as $\overline{\alpha'_{sw} \times swflx'}$, where α'_{sw} is the monthly anomaly of the shortwave absorption rate, defined as shortwave heating divided by shortwave flux, and the $swflx'$ is the monthly anomaly of shortwave flux. The α'_{sw} is strongly controlled by the monthly chlorophyll anomaly. The MNSH showed the summer shortwave cooling effect because the covariance between chlorophyll and shortwave flux variability is strongly negative, while this covariance is weakly positive in spring, which results in a net cooling effect by NT_{sw}. The cooling effect of NT_{sw} is induced by positive ice–phytoplankton coupling in summer, resulting from the covariability between sea ice and chlorophyll anomalies. For the interannual high sea ice year, the mixing of the Arctic Ocean increases relatively, which leads to a positive chlorophyll anomaly in the nutrient-limiting conditions in summer. Meanwhile, the high sea ice conditions reflect the shortwave flux, which leads to a negative shortwave flux anomaly. Thus, two characteristics of the negative shortwave flux and positive chlorophyll anomalies induce a negative MNSH in summer.

However, the MNSH will be changed under the greenhouse warming conditions. Figure 5 shows the patterns of the MNSH of BGC.on.1×CO_2 and BGC.on.2×CO_2 in spring (March and April) and summer (July and August). In spring under present-day climate conditions (Fig. 5a), the MNSH shows both shortwave cooling and heating patterns along the edge of the sea ice near Barents Sea, Bering, and Fram Strait. In summer under present-day climate conditions, the MNSH shows the overall cooling pattern in Arctic Ocean, which is in contrast to the patterns observed in spring.

Part I suggested that the summer shortwave cooling effect overwhelms the spring shortwave heating effect, which was

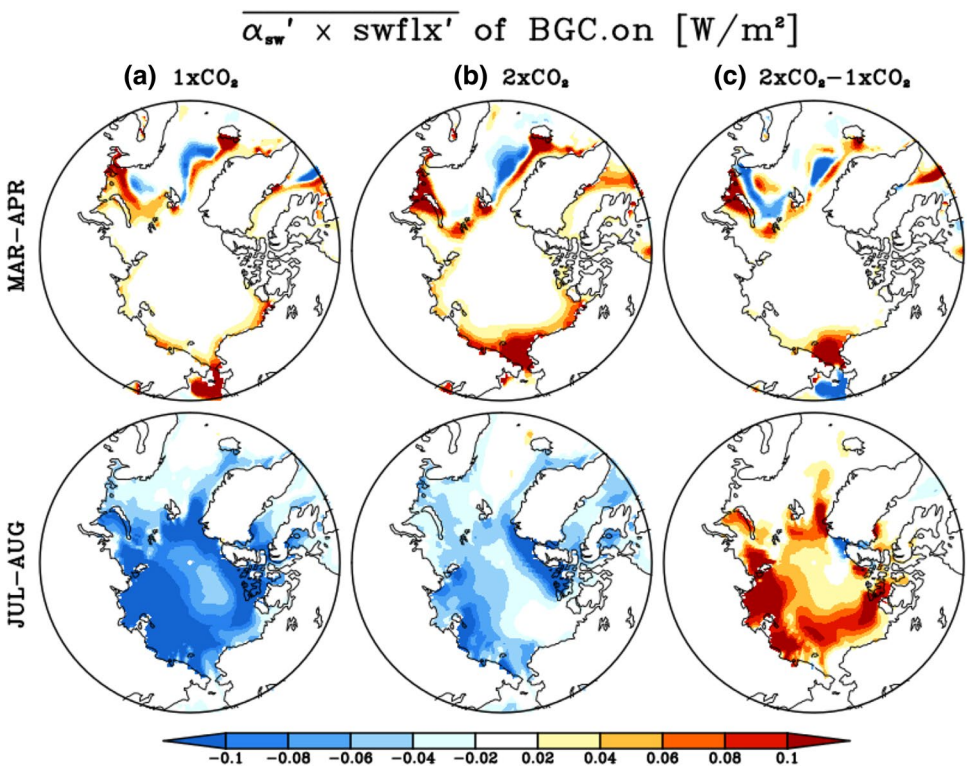

Fig. 5 The time mean of nonlinear shortwave heating (MNSH) $\overline{\alpha'_{sw} \times swflx'}$ averaged up to 30-m depth in spring (March–April in upper row) and summer (July–August in below row) under **a** present-day climate, **b** future climate, and **c** difference between future and present-day climate

called rectification effect of NT_{sw}. Interestingly, the rectification effect of NT_{sw} is gradually reduced under future climate conditions (Fig. 5b). In spring under future climate conditions, the MNSH still shows both shortwave cooling and heating patterns near marginal sea ice zones that are shifted poleward due to retreat of the sea ice edge. The difference between shortwave heating under present-day and future climate conditions shows the positive pattern being shifted from the Bering Sea to the Chukchi Sea and from the Barents Sea to the Barents-Kara Seas border (Fig. 5c). In summer under future climate conditions, the MNSH shows an overall shortwave cooling pattern in the Arctic Ocean (Fig. 5b). However, the magnitude of this negative pattern in the MNSH is substantially weakened basin-wide in the Arctic Ocean in summer (Fig. 5c). Both warming patterns of the MNSH differences in spring and summer indicates anomalous shortwave heating, which can enhance Arctic amplification. Thus, the warming impact of interactive chlorophyll shown in Figs. 3 and 4 might be explained by a weakening of the rectification effect of NT_{sw} to a large extent.

Figure 6 shows the seasonal evolution of the MNSH $\overline{\alpha'_{sw} \times swflx'}$ in the Arctic Ocean. In the present-day climate, it is clear that the amplitude of positive MNSH in spring is relatively weak but the amplitude of negative MNSH in summer is relatively strong (black line in Fig. 6). The maximum in spring and the minimum in summer appear one month earlier under greenhouse warming conditions (red line in Fig. 6). The stratified Arctic Ocean and sea ice melting due

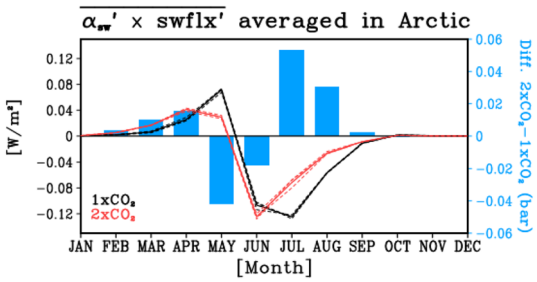

Fig. 6 The MNSH $\overline{\alpha'_{sw} \times swflx'}$ up to 30-m depth in the Arctic Ocean (> 65°N) in individual ensembles (dashed line) and ensemble mean (straight line) of present-day climate (1×CO_2; black line), future climate (2×CO_2; red line), and ensemble mean difference between future and present-day climate (blue bar)

to greenhouse warming alters the timing of the two peaks by changing limiting conditions of light and nutrients. The light limiting condition in spring is relatively weakened by decreased sea ice concentration and thickness. In addition, the nutrient-limiting condition in early summer is relatively intensified during May–June by nutrient depletion (Fig. 2), which leads to faster oligotrophic onset. However, the strong negative MNSH during July and August is gradually diminished. The coldest peak of the MNSH in July gradually decreases from −0.12 W/m^2 to − 0.07 W/m^2 (− 43.6%). The annual mean MNSH decreases from −0.016 W/m^2 to

-0.011 W/m^2 (-31.3%), which represents a weakening of rectification effect of NT_{sw} in the future climate.

To examine the mechanism for change in the MNSH during boreal summer (JJA), the sea ice and chlorophyll variabilities in present-day and future climate are shown in Fig. 7a, b. Under greenhouse warming conditions, the sea ice variability gradually decreases from 11.4% in present-day to 6.9% in the future climate (Fig. 7a). The weakened sea ice variability can be linked to a weakening of ice–phytoplankton coupling. The chlorophyll variability is also gradually weakened by about 21% from 0.14 mg/m^3 in present-day to 0.11 mg/m^3 in the future climate in the Arctic Ocean (Fig. 7b). In addition to the weakened ice–phytoplankton coupling, the stabilized Arctic Ocean in the future climate, lower efficiency of upwelling nutrient due to lower nitrate concentration than present-day climate, can partly contribute to the decreased chlorophyll variability. Consequently, both weakening of chlorophyll and sea ice variabilities reduce the covariance between chlorophyll and sea ice concentration anomalies basin-wide in the Arctic Ocean (Fig. 7c). Because the sea ice directly controls the shortwave flux via high surface albedo, sea ice and shortwave flux are negatively correlated. Provided that the covariance between sea ice and chlorophyll variabilities is reduced, we can expect that the covariance between shortwave flux and chlorophyll, which determines the amplitude of the MNSH, will be reduced. Thus, the reduced covariance between sea ice and chlorophyll results in a reduction of the MNSH in summer.

Interannual variability of chlorophyll is mostly reduced in summer under greenhouse warming conditions (Fig. 8a), with the chlorophyll variability in July being especially weakened by about 30.3% from 0.041 mg/m^3 in present-day to 0.029 mg/m^3 in the future climate. The nutrient conditions are lowest in summer as the seasonal cycle of nitrate represent a minimum. In this condition, the same amount of the ocean mixing under greenhouse warming could have a low efficiency to carry nitrate in subsurface out to the surface compared to present-day climate. The sea ice reduction and in turn nutrient depletion can effectively reduce chlorophyll variability in this season due to enhanced oligotrophic condition under greenhouse warming conditions. In March and April, however, sea ice reduction enhances the chlorophyll variability due to the light limiting condition released by more shortwave flux input.

The covariance between chlorophyll and shortwave flux anomalies is strongly suppressed in summer (Fig. 8b). Both decreases of shortwave and chlorophyll variabilities lead to a decrease in the MNSH (i.e., weakening of the summer shortwave cooling). Consequently, the interactive chlorophyll variability in the future climate absorbs more shortwave radiation than that in the present-day climate. This reduces the cooling effect by rectification of NT_{sw} in the future climate.

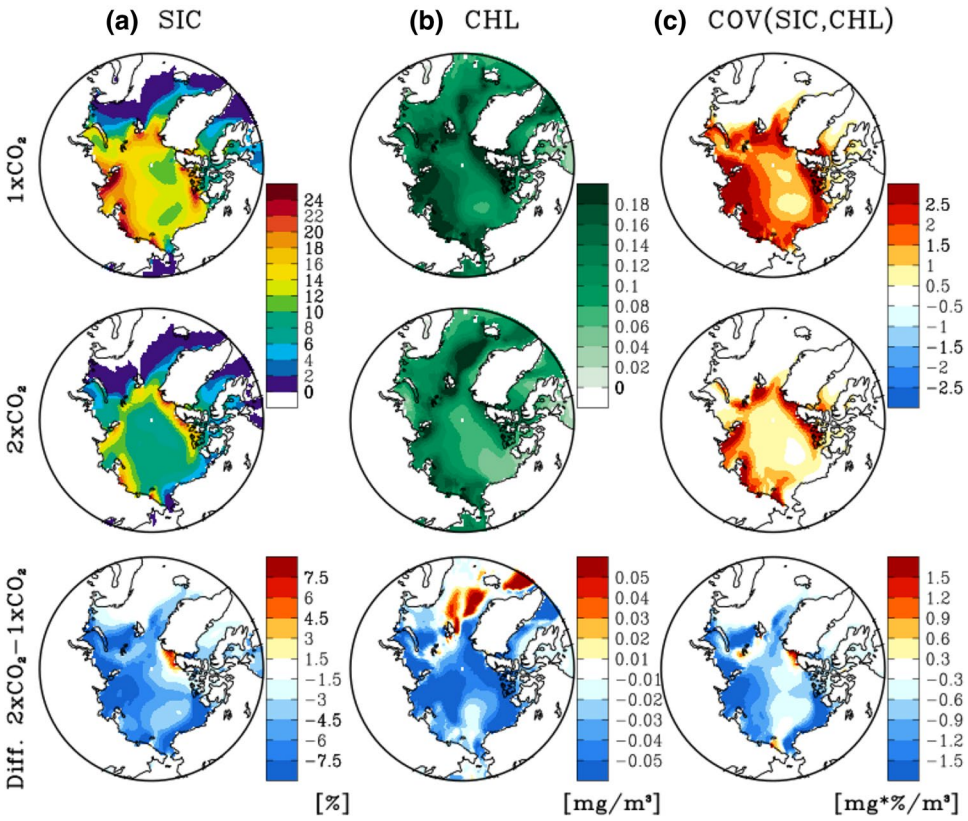

Fig. 7 In the present-day (top) and future climates (middle), **a** sea ice concentration, **b** chlorophyll variabilities (defined as 1 standard deviation), and **c** covariance coefficients between sea ice concentration and chlorophyll in JJA. The difference between future and present-day climates are shown in bottom rows

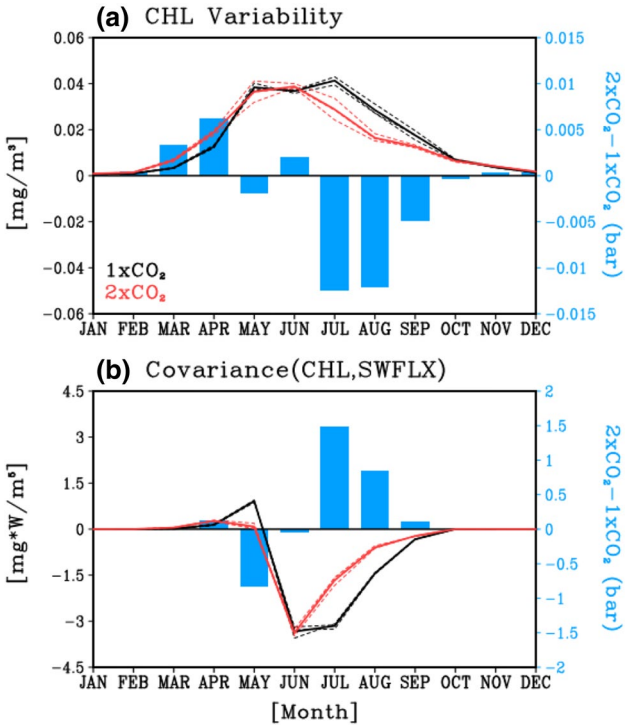

Fig. 8 The present-day climate (BGC.on.1×CO_2; black), future climate (BGC.on.2×CO_2; red), and their difference (BGC.on.2×CO_2 minus BGC.on.1×CO_2; blue) for **a** chlorophyll variability (defined as 1 standard deviation) and **b** covariance between chlorophyll and shortwave flux in the Arctic Ocean (> 65°N)

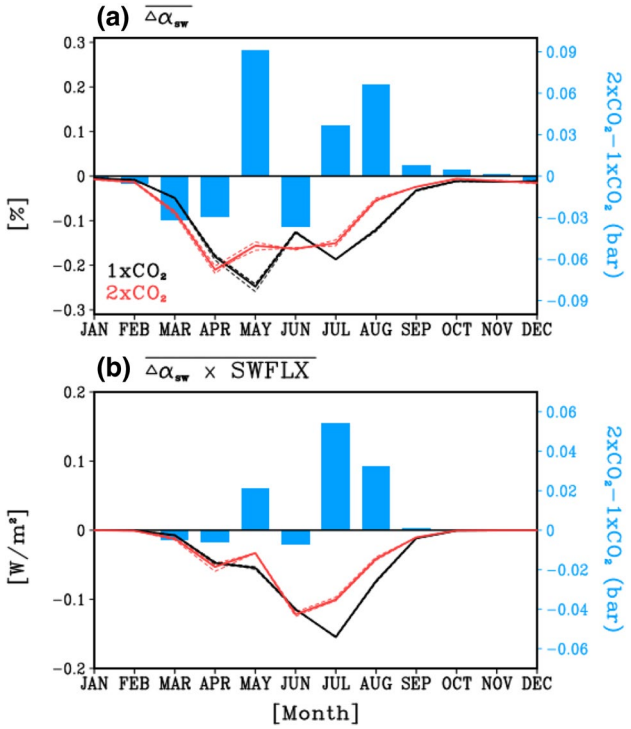

Fig. 9 The ideal cases of **a** the time mean shortwave absorption rate difference $\overline{\Delta\alpha_{sw}}$ (Δ is BGC.on minus BGC.off) and **b** nonlinear term of the shortwave absorption rate NF_α estimated by idealized $\overline{\Delta\alpha_{sw} \times swflx}$ in the present-day (black) and future climate (red) in the Arctic Ocean (> 65°N). The blue bar shows the difference of **a** idealized $\overline{\Delta\alpha_{sw}}$ and **b** idealized $\overline{\Delta\alpha_{sw} \times swflx}$ of the future climate minus that of the present-day climate. In this ideal case, calculations of α_{sw} are based on the varying chlorophyll and climatological chlorophyll in BGC.on and BGC.off. The other factors, shortwave flux, visible fraction in shortwave flux, and column thickness of the ocean layer, were fixed into ideal cases as BGC.on.1×CO_2

In addition to NT_{sw} effect, Part I suggested that chlorophyll variability itself contributes to the significant cooling effects via the other nonlinear rectification in the present-day climate (NF_α). The time mean difference of α_{sw} ($\Delta\overline{\alpha_{sw}}$) between the cases of interactive chlorophyll variability and non-varying chlorophyll was negative so MMSH term expressed as $\overline{\alpha_{sw}} \times \overline{swflx}$ had a cooling effect. Because the α_{sw} is approximately determined by an exponential function of chlorophyll ($1 - \exp^{-[chl]}$, Eq. 5 in Manizza et al. 2005), the change in α_{sw} corresponding to the changing chlorophyll is nonlinear. Note that most of chlorophyll-based shortwave heating schemes including Manizza et al. (2005) and others (Marzeion et al. 2005; Lengaigne et al. 2007; Vichi et al. 2007) are approximately determined by an exponential function based on Morel (1988) and Lambert–Beer's Law. The α_{sw} nonlinearity indicates that the magnitude of absorption rate response to a positive chlorophyll anomaly is smaller than that of the responses to a negative chlorophyll anomaly. Thus, chlorophyll variability generates the negative $\Delta\overline{\alpha_{sw}}$ compared to non-varying chlorophyll, that significantly rectifies the cold Arctic mean state via the cooling effect of the NF_α.

We estimated the effect of $\Delta\overline{\alpha_{sw}}$ in the present-day and future climates (Fig. 9a). Both $\Delta\overline{\alpha_{sw}}$ were generally negative in all months implying a lower absorption rate associated with interactive chlorophyll variability regardless of climate state. Under greenhouse warming conditions, however, the negative $\Delta\overline{\alpha_{sw}}$ changes slightly. Less negative $\Delta\overline{\alpha_{sw}}$ is observed when future chlorophyll variabilities are weakened in May, July, and August, while more negative $\Delta\overline{\alpha_{sw}}$ is observed when future chlorophyll variabilities are enhanced in March, April, and June, which is consistent with the result of changes of chlorophyll variability presented in Fig. 8a. The cooling impact of $\Delta\overline{\alpha_{sw}}$ (i.e., NF_α) is strongest in July and August due to the strong seasonal amplitude of shortwave flux. In this regard, changes in the $\Delta\overline{\alpha_{sw}}$ in summer might be most effective.

We calculate the $\overline{\Delta\alpha_{sw} \times swflx}$ for the present-day and future climates (Fig. 9b). Both $\overline{\Delta\alpha_{sw} \times swflx}$ are generally negative in all months, implying the cooling impact of the NF_α is dominant regardless of climate state. Under greenhouse warming conditions, however, the cooling impact is reduced from −0.11 to − 0.07 W/m^2 (− 38.0%) in July

and August due to a weakened $\Delta\overline{\alpha_{sw}}$. The annual mean $\overline{\Delta\alpha_{sw} \times swflx}$ decreases from −0.038 to − 0.031 W/m^2 (− 19.5%). This represents a weakening of the rectification effect of the NF_α in the future climate. The result of this section implies that reductions of the nonlinear rectification effects (i.e., NT_{sw} and NF_α) can lead to additional shortwave heating source in the future Arctic summer, which couldn't be explained by the linear process of decreased mean chlorophyll and in turn the expected shortwave cooling.

4 Summary and discussion

Using a state-of-the-art ESM, this study shows that interactive chlorophyll variability plays a role in enhancing the amplification of Arctic warming. The major finding in this paper is that the cooling impact of two nonlinear rectification effects of interactive chlorophyll variability in the present-day climate will be weakened in the future climate. Decreased sea ice variability directly affects the weakening of rectification effect of NT_{sw} by a weakening of the covariance between sea ice and chlorophyll anomalies. In addition, the decreased sea ice variability indirectly affects the rectification effect of the NF_α because sea ice partly controls ocean mixing variability and in turn chlorophyll variability. The weakening of sea ice variability reduces chlorophyll variability, which affects the weakening of the rectification effect of the NF_α. In this study, the decreased interannual chlorophyll variability amplifies Arctic surface warming (+ 10% in both regions) and sea ice melting (− 13% and − 10%) in Kara-Barents Seas and the East Siberian-Chukchi Seas in boreal winter, respectively. Thus, sea ice melting and its interaction with chlorophyll can significantly amplify the Arctic warming by the weakening of both nonlinear rectification effects of interactive chlorophyll variability in the future.

This study used long integrations of GFDL CM2.1 and examined the impact of interactive chlorophyll at the equilibrium state of a doubling in the atmospheric CO_2 concentrations in the future climate. This approach using sensitivity experiments refined the robust result reported in P15 that interactive chlorophyll enhances oceanic shortwave heating and in turn Arctic warming. P15 suggested that interactive chlorophyll amplifies the Arctic warming by increased mean chlorophyll concentrations. However, Part I suggested that the limiting factors of chlorophyll are light availability in spring and nutrient availability in summer. This new insight regarding the seasonal dependency of limiting factors for chlorophyll led to a better understanding of chlorophyll response by looking at the physical and biogeochemical properties under greenhouse warming conditions. We found that sea ice retreat leads to a positive chlorophyll response in spring due to increased incoming solar radiation but a negative chlorophyll response due to nutrient depletion in a warmer Arctic climate and in turn a more stratified Arctic Ocean. This consequently led to the conclusion that these changes in chlorophyll levels and related physical properties affect the impact of nonlinear rectification effects (i.e., NT_{sw} and NF_α). Therefore, the present study offers new insight into Arctic climate sensitivity by biogeophysical feedback which should not only be considered by the change in mean chlorophyll concentration, but also by the change in interannual chlorophyll variability and its interaction between the other physical properties in the Arctic Ocean.

In addition, P15 estimated the impact of the future chlorophyll during a 100-year run, which showed a similar amplitude of positive chlorophyll response in spring and a smaller amplitude of negative chlorophyll response in summer. Thus, the results reported in P15 were primarily associated with the major impact of the mean chlorophyll difference. As stratification of the surface water progressed, the present study, which was conducted with a 200-years run, suggests the negative chlorophyll response in summer is stronger than that reported in P15, which contributes to the negative annual mean chlorophyll response. Nevertheless, Arctic warming was amplified by biogeophysical feedback under reduced biological activity. In this case, we should consider the changes of nonlinear rectification effects of chlorophyll variability to understand how interactive chlorophyll enhances Arctic warming, as discussed in the present study.

While this study pointed out the effect of interactive chlorophyll variability on Arctic climate change, there are some caveats to consider. First, the chlorophyll in the Arctic sea ice zone is expected to suffer a reduction in mean concentration, but there is still strong inter-model diversity with wide range from positive to negative chlorophyll responses (Cabré et al. 2015). Thus, the sensitivity to an interactive chlorophyll could be diverse in the Arctic region. Also, it is hard to clearly estimate the diversity of shortwave heating induced by chlorophyll variability using CMIP5 models. Some ESMs (e.g. HadGEM2-ES(CC), MIROC-ESM, MRI-ESM, MPI-ESM, and CNRM-CM5) either do not include or turn off the shortwave heating scheme associated with interactive chlorophyll so they are missing the biogeophysical feedback in their simulations. These biogeophysical feedbacks can only be evaluated in a few ESMs, which include these biogeophysical coupling in their simulations: GFDL-ESM2M, GFDL-ESM2G, IPSL-CM5A-LR, IPSL-CM5A-MR, and IPSL-CM5B-LR. Investigating the relationship between chlorophyll and shortwave flux in both historical and Representative Concentration Pathways 4.5 (RCP4.5) scenarios in these CMIP5 ESMs (Fig. 10a) indicate a decreased covariance in summer. This decreased covariance between chlorophyll and shortwave flux may give an additional shortwave heating source, as shown in the present study. Also, this

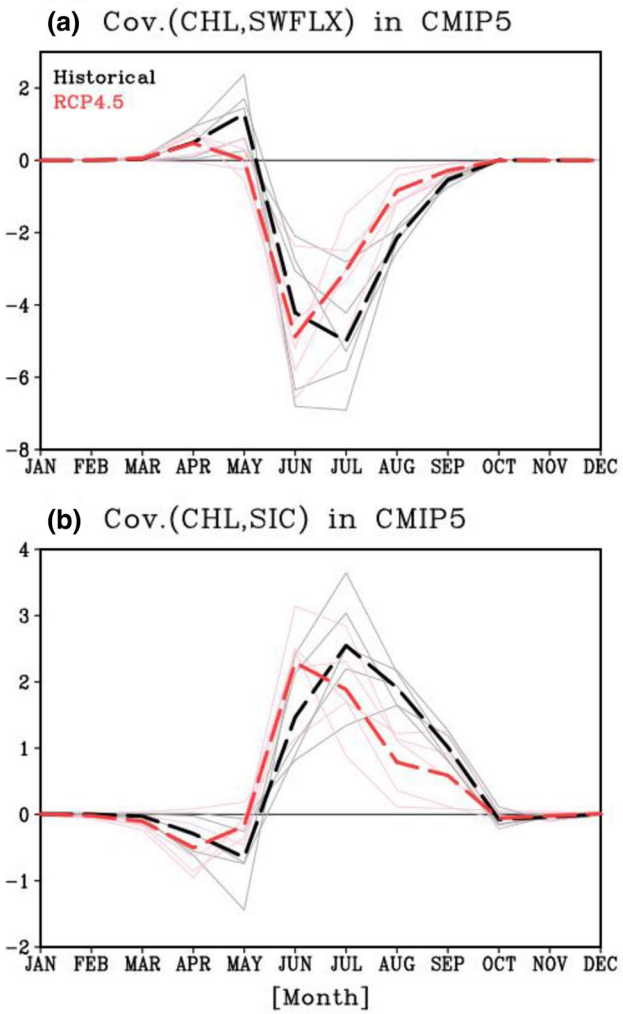

Fig. 10 The covariance **a** between chlorophyll and sea ice, **b** between chlorophyll and shortwave flux in the historical and RCP4.5 runs in the five CMIP5 ESMs (e.g. GFDL-ESM2M, GFDL-ESM2G, IPSL-CM5A-LR, IPSL-CM5A-MR, and IPSL-CM5B-LR). Historical run and RCP4.5 scenarios are analyzed over 40 years during 1961–2000 and 2061–2100 years

decreasing covariance is closely related to the weakening of ice–phytoplankton coupling in summer (Fig. 10b). This result suggests a possibility of a warming impact from chlorophyll variability in the other models, which supports our findings. However, because it is based on just a few models, with some of them being from the same modeling group, further sensitivity tests with different models are needed to quantify the contrasting impacts between the reduced warming role of mean chlorophyll levels and the reduced cooling role of nonlinear rectification effects in RCP4.5.

Second, the interaction between climate variability and biogeochemical processes such as riverine nutrient, atmospheric deposition (Gruber and Galloway 2008), and iron fluxes (Klunder et al. 2012) were excluded from our experimental set-up. The coupling processes of nutrients can modulate not only mean chlorophyll, but also chlorophyll interannual variability. Then, the sensitivity of impact of chlorophyll variability in the present-day and future climates could be different. The interaction between climate variability and biogeochemical processes should be included in the ESM to refine projections of the future Arctic climate sensitivity.

The external forcing of nutrient fluxes prescribed by pre-industrial fluxes of nitrogen and iron (Horowitz et al. 2003; Green et al. 2004; Fan et al. 2006) are another caveat of this study. Nutrient depletion via ocean stratification under greenhouse warming conditions enhances oligotrophic condition. The initial condition of nutrients and their fluxes will determine decreasing trends of the chlorophyll and future chlorophyll concentrations. The shortwave absorption rate is obviously affected by chlorophyll concentrations. Therefore, the impact of interactive chlorophyll by the anthropogenic nutrient external forces should be evaluated.

The primary findings of Parts I and II are associated with the two nonlinear rectification effects of chlorophyll variability on the Arctic climate mean state. This suggests that previously reported impacts associated with biogeophysical feedback and their mechanisms are not only driven by the changes in mean chlorophyll concentrations, but are also significantly driven by changes in interannual chlorophyll variability. In long-term simulations of CMIP5 ESMs, the chlorophyll variability and their biogeophysical feedbacks can contribute to more realistic simulations such as improving the Arctic sea ice mean state (Part I) and decreasing trend of sea ice in September (P15). The present study investigates the Arctic warming due to the interactive chlorophyll and suggests detailed mechanism including nonlinear processes associated with two nonlinear rectification effects. We showed the CMIP5 ESMs represent the cooling effect of the two nonlinear rectification effect in Part I, and their possible future changes in the present study. However, our present study has a clear limitation to analyze the detail processes of the CMIP5 simulation due to the data availability issue, so more detail analyses in the other models will be needed in a further study.

Acknowledgements This work is supported by the project titled '[Korea-Arctic Ocean Observing System (K-AOOS), KOPRI, 20160245]', funded by the MOF, Korea, and the National Research Foundation of Korea (NRF-2018R1A5A1024958). H.-G. Lim is supported by Hyundai Motor Chung Mong-Koo Foundation.

References

Ardyna M, Babin M, Gosselin M, Devred E, Rainville L, Tremblay J (2014) Recent Arctic Ocean sea ice loss triggers novel fall phytoplankton blooms. Geophys Res Lett 41:6207–6212

Arrigo KR, van Dijken G, Pabi S (2008) Impact of a shrinking Arctic ice cover on marine primary production. Geophys Res Lett 35 https://doi.org/10.1029/2008gl035028

Arrigo KR, Perovich DK, Pickart RS, Brown ZW, Van Dijken GL, Lowry KE, Mills MM, Palmer MA, Balch WM, Bahr F (2012) Massive phytoplankton blooms under Arctic sea ice. Science 336:1408–1408

Arrigo KR, Perovich DK, Pickart RS, Brown ZW, van Dijken GL, Lowry KE, Mills MM, Palmer MA, Balch WM, Bates NR, Benitez-Nelson CR, Brownlee E, Frey KE, Laney SR, Mathis J, Matsuoka A, Greg Mitchell B, Moore GWK, Reynolds RA, Sosik HM, Swift JH (2014) Phytoplankton blooms beneath the sea ice in the Chukchi sea. Deep Sea Res Part II 105:1–16. https://doi.org/10.1016/j.dsr2.2014.03.018

Behrenfeld MJ, O'Malley RT, Siegel DA, McClain CR, Sarmiento JL, Feldman GC, Milligan AJ, Falkowski PG, Letelier RM, Boss ES (2006) Climate-driven trends in contemporary ocean productivity. Nature 444:752. https://doi.org/10.1038/nature05317. https://www.nature.com/articles/nature05317#supplementary-information

Boé J, Hall A, Qu X (2009) September sea–ice cover in the Arctic Ocean projected to vanish by 2100. Nat Geosci 2:341. https://doi.org/10.1038/ngeo467

Bopp L, Resplandy L, Orr JC, Doney SC, Dunne JP, Gehlen M, Halloran P, Heinze C, Ilyina T, Séférian R, Tjiputra J, Vichi M (2013) Multiple stressors of ocean ecosystems in the 21st century: projections with CMIP5 models. Biogeosciences 10:6225–6245. https://doi.org/10.5194/bg-10-6225-2013

Boyce DG, Lewis MR, Worm B (2010) Global phytoplankton decline over the past century. Nature 466:591. https://doi.org/10.1038/nature09268. https://www.nature.com/articles/nature09268#supplementary-information

Cabré A, Marinov I, Leung S (2015) Consistent global responses of marine ecosystems to future climate change across the IPCC AR5 earth system models. Clim Dyn 45:1253–1280

Comiso JC (2003) Warming trends in the Arctic from clear sky satellite observations. J Clim 16:3498–3510 https://doi.org/10.1175/1520-0442(2003)016%3C3498:wtitaf%3E2.0.co;2

Comiso JC, Parkinson CL, Gersten R, Stock L (2008) Accelerated decline in the Arctic sea ice cover. Geophys Res Lett. https://doi.org/10.1029/2007GL031972

Deser C, Haiyan T (2013) Recent Trends in Arctic Sea Ice and the Evolving Role of Atmospheric Circulation Forcing, 1979–2007. In: Arctic Sea ice decline: observations, projections, mechanisms, and implications. Geophysical Monograph Series. https://doi.org/10.1029/180GM03

Doney SC, Ruckelshaus M, Duffy JE, Barry JP, Chan F, English CA, Galindo HM, Grebmeier JM, Hollowed AB, Knowlton N, Polovina J, Rabalais NN, Sydeman WJ, Talley LD (2012) Climate change impacts on marine ecosystems. Ann Rev Mar Sci 4:11–37. https://doi.org/10.1146/annurev-marine-041911-111611

Dunne JP, John JG, Shevliakova E, Stouffer RJ, Krasting JP, Malyshev SL, Milly PCD, Sentman LT, Adcroft AJ, Cooke W, Dunne KA, Griffies SM, Hallberg RW, Harrison MJ, Levy H, Wittenberg AT, Phillips PJ, Zadeh N (2013) GFDL's ESM2 global coupled climate–carbon earth system models. Part II: carbon system formulation and baseline simulation characteristics. J Clim 26:2247–2267. https://doi.org/10.1175/jcli-d-12-00150.1

Dunstan PK, Foster SD, King E, Risbey J, O'Kane TJ, Monselesan D, Hobday AJ, Hartog JR, Thompson PA (2018) Global patterns of change and variation in sea surface temperature and chlorophyll a. Sci Rep 8:14624. https://doi.org/10.1038/s41598-018-33057-y

Fan S-M, Moxim WJ, Levy H (2006) Aeolian input of bioavailable iron to the ocean. Geophys Res Lett 33:L07602. https://doi.org/10.1029/2005GL024852

Frey KE, Moore GWK, Cooper LW, Grebmeier JM (2015) Divergent patterns of recent sea ice cover across the Bering, Chukchi, and Beaufort seas of the Pacific Arctic Region. Prog Oceanogr 136:32–49. https://doi.org/10.1016/j.pocean.2015.05.009

Green PA, Vörösmarty CJ, Meybeck M, Galloway JN, Peterson BJ, Boyer EW (2004) Pre-industrial and contemporary fluxes of nitrogen through rivers: a global assessment based on typology. Biogeochemistry 68:71–105. https://doi.org/10.1023/b:biog.0000025742.82155.92

Griffies SM (2012) Elements of the modular ocean model (MOM). NOAA Geophysical Fluid Dynamics Laboratory, Princeton

Gruber N, Galloway JN (2008) An Earth-system perspective of the global nitrogen cycle. Nature 451:293. https://doi.org/10.1038/nature06592

Haas C, Pfaffling A, Hendricks S, Rabenstein L, Etienne JL, Rigor I (2008) Reduced ice thickness in arctic transpolar drift favors rapid ice retreat. Geophys Res Lett. https://doi.org/10.1029/2008GL034457

Holland MM, Serreze MC, Stroeve J (2010) The sea ice mass budget of the Arctic and its future change as simulated by coupled climate models. Clim Dyn 34:185–200

Horowitz LW, Walters S, Mauzerall DL, Emmons LK, Rasch PJ, Granier C, Tie X, Lamarque J-F, Schultz MG, Tyndall GS, Orlando JJ, Brasseur GP (2003) A global simulation of tropospheric ozone and related tracers: description and evaluation of MOZART, version 2. J Geophys Res Atmos. https://doi.org/10.1029/2002JD002853

Kashiwase H, Ohshima KI, Nihashi S, Eicken H (2017) Evidence for ice–ocean albedo feedback in the Arctic Ocean shifting to a seasonal ice zone. Sci Rep 7:8170. https://doi.org/10.1038/s41598-017-08467-z

Klunder MB, Bauch D, Laan P, de Baar HJW, van Heuven S, Ober S (2012) Dissolved iron in the Arctic shelf seas and surface waters of the central Arctic Ocean: impact of Arctic river water and ice-melt. J Geophys Res Oceans 117:C01027. https://doi.org/10.1029/2011JC007133

Kwok R, Rothrock DA (2009) Decline in Arctic sea ice thickness from submarine and ICESat records: 1958–2008. Geophys Res Lett. https://doi.org/10.1029/2009GL039035

Lawrence J, Popova E, Yool A, Srokosz M (2015) On the vertical phytoplankton response to an ice-free Arctic Ocean. J Geophys Res Oceans 120:8571–8582. https://doi.org/10.1002/2015JC011180

Lengaigne M, Menkes C, Aumont O, Gorgues T, Bopp L, André J-M, Madec G (2007) Influence of the oceanic biology on the tropical Pacific climate in a coupled general circulation model. Clim Dyn 28:503–516. https://doi.org/10.1007/s00382-006-0200-2

Lengaigne M, Madec G, Bopp L, Menkes C, Aumont O, Cadule P (2009) Bio-physical feedbacks in the Arctic Ocean using an Earth system model. Geophys Res Lett 36

Lim H-G, Kug J-S, Park J-Y (2018a) Biogeophysical feedback of phytoplankton on the Arctic climate. Part I: Impact of nonlinear rectification of interactive chlorophyll variability in the present-day climate. Clim Dyn. https://doi.org/10.1007/s00382-018-4450-6

Lim H-G, Park J-Y, Kug J-S (2018b) Impact of chlorophyll bias on the tropical Pacific mean climate in an earth system model. Clim Dyn. https://doi.org/10.1007/s00382-017-4036-8

Liu J, Song M, Horton RM, Hu Y (2013) Reducing spread in climate model projections of a September ice-free Arctic. Proc Natl Acad Sci 110:12571–12576. https://doi.org/10.1073/pnas.1219716110

Manizza M, Le Quéré C, Watson AJ, Buitenhuis ET (2005) Bio-optical feedbacks among phytoplankton, upper ocean physics and sea–ice in a global model. Geophys Res Lett 32:L05603. https://doi.org/10.1029/2004GL020778

Marzeion B, Timmermann A, Murtugudde R, Jin F-F (2005) Biophysical feedbacks in the tropical Pacific. J Clim 18:58–70

Maslanik JA, Fowler C, Stroeve J, Drobot S, Zwally J, Yi D, Emery W (2007) A younger, thinner Arctic ice cover: increased potential for rapid, extensive sea–ice loss. Geophys Res Lett 34:L24501. https://doi.org/10.1029/2007GL032043

Min S-K, Son S-W, Seo K-H, Kug J-S, An S-I, Choi Y-S, Jeong J-H, Kim B-M, Kim J-W, Kim Y-H, Lee J-Y, Lee M-I (2015) Changes in weather and climate extremes over Korea and possible causes: a review. Asia-Pacific J Atmos Sci 51:103–121. https://doi.org/10.1007/s13143-015-0066-5

Morel A (1988) Optical modeling of the upper ocean in relation to its biogenous matter content(case I waters). J Geophys Res 93:749–710

Morel A, Antoine D (1994) Heating rate within the upper ocean in relation to its bio-optical state. J Phys Oceanogr 24:1652–1665

Nicolaus M, Katlein C, Maslanik J, Hendricks S (2012) Changes in Arctic sea ice result in increasing light transmittance and absorption. Geophys Res Lett. https://doi.org/10.1029/2012GL053738

Overland JE, Wang M (2013) When will the summer Arctic be nearly sea ice free? Geophys Res Lett 40:2097–2101. https://doi.org/10.1002/grl.50316

Park JY, Kug JS, Badera J, Rolph R, Kwon M (2015) Amplified Arctic warming by phytoplankton under greenhouse warming. P Natl Acad Sci USA 112:5921–5926. https://doi.org/10.1073/pnas.1416884112

Peralta-Ferriz C, Woodgate RA (2015) Seasonal and interannual variability of pan-Arctic surface mixed layer properties from 1979 to 2012 from hydrographic data, and the dominance of stratification for multiyear mixed layer depth shoaling. Prog Oceanogr 134:19–53. https://doi.org/10.1016/j.pocean.2014.12.005

Perovich DK, Light B, Eicken H, Jones KF, Runciman K, Nghiem SV (2007) Increasing solar heating of the Arctic Ocean and adjacent seas, 1979–2005: attribution and role in the ice-albedo feedback. Geophys Res Lett 34

Perovich DK, Jones K, Light B, Eicken H, Markus T, Stroeve JC, Lindsay R (2011) Solar partitioning in a changing Arctic sea–ice cover. https://doi.org/10.3189/172756411795931543

Popova EE, Yool A, Coward AC, Dupont F, Deal C, Elliott S, Hunke E, Jin M, Steele M, Zhang J (2012) What controls primary production in the Arctic Ocean? Results from an intercomparison of five general circulation models with biogeochemistry. J Geophys Res Oceans 117:C00D12. https://doi.org/10.1029/2011JC007112

Sarmiento JL, Slater R, Barber R, Bopp L, Doney SC, Hirst AC, Kleypas J, Matear R, Mikolajewicz U, Monfray P, Soldatov V, Spall SA, Stouffer R (2004) Response of ocean ecosystems to climate warming. Global Biogeochem Cycles. doi:https://doi.org/10.1029/2003GB002134

Serreze MC, Holland MM, Stroeve J (2007) Perspectives on the Arctic's shrinking sea–ice cover. Science 315:1533–1536. https://doi.org/10.1126/science.1139426

Stroeve JC, Kattsov V, Barrett A, Serreze M, Pavlova T, Holland M, Meier WN (2012) Trends in Arctic sea ice extent from CMIP5, CMIP3 and observations. Geophys Res Lett 39:L16502. https://doi.org/10.1029/2012GL052676

Tremblay J-É, Gagnon J (2009) The effects of irradiance and nutrient supply on the productivity of Arctic waters: a perspective on climate change. In: Influence of climate change on the changing arctic and sub-arctic conditions. Springer, pp 73–93

Vancoppenolle M, Bopp L, Madec G, Dunne J, Ilyina T, Halloran PR, Steiner N (2013) Future Arctic Ocean primary productivity from CMIP5 simulations: uncertain outcome, but consistent mechanisms. Global Biogeochem Cycles 27:605–619. https://doi.org/10.1002/gbc.20055

Vichi M, Pinardi N, Masina S (2007) A generalized model of pelagic biogeochemistry for the global ocean ecosystem. Part I: Theory. J Mar Syst 64:89–109

Wang J, Zhang J, Watanabe E, Ikeda M, Mizobata K, Walsh JE, Bai X, Wu B (2009) Is the Dipole Anomaly a major driver to record lows in Arctic summer sea ice extent? Geophys Res Lett 36

Wassmann P, Reigstad M (2011) Future Arctic Ocean seasonal ice zones and implications for pelagic-benthic coupling

Winder M, Sommer U (2012) Phytoplankton response to a changing climate. Hydrobiologia 698:5–16. https://doi.org/10.1007/s10750-012-1149-2